Extreme abundance of ammonoids in mass accumulations from the Late Devonian of the Moroccan Anti-Atlas

MERLE GREIF, JAMES H. NEBELSICK, and CHRISTIAN KLUG

Greif, M., Nebelsick, J.H., and Klug, C. 2022. Extreme abundance of ammonoids in mass accumulations from the Late Devonian of the Moroccan Anti-Atlas. *Acta Palaeontologica Polonica* 67 (3): 667–684.

The eastern Anti-Atlas is renowned for its highly fossiliferous outcrops of Devonian rocks. Ammonoids occur in rock-forming numbers at many localities in the Tafilalt and Maïder. This study addresses the questions of how many ammonoids are preserved within a standardized area as well as over the whole Tafilalt and Maïder basins, and how these mass occurrences formed. Five samples from the Tafilalt and Maïder were analysed. The ammonoids contained therein were prepared, measured and counted as a base for estimates of the orders of magnitude of the total number of preserved ammonoids and their biomass within the respective Famennian strata in the eastern Anti-Atlas. Two samples were stratigraphically assigned to the lower Famennian, two samples to the middle Famennian and one sample to the upper Famennian. For these samples, estimates for a standardized area of 1 km^2 and a layer thickness of 100 mm lie between 19.9×10^9 and 1.25×10^{10} ammonoids. The estimated numbers for the whole study area with a retrodeformed size of 15 512.5 km^2 and a sediment thickness of 100 mm, ranges from 30.9×10^{13} to 19.4×10^{14} ammonoids and a annual accumulation of 15.4×10^9 to 97.1×10^9 ammonoid conchs. This corresponds to a annual total palaeo-biomass that ranges from 25 954 t to 47 058 t within the whole study area and from 1.67 t to 3.03 t within an area of 1 km^2. Based on these results and size-distribution in the samples, the ecological role of the small and highly abundant, subspherical ammonoids from the early and middle Famennian is discussed and reproductive rates are estimated. With ca. 230 eggs produced by an adult female, cheiloceratids and small maeneceratids from the early Famennian deposits are at the lower end of ammonoid reproductive rates.

Key words: Cephalopoda, Ammonoidea, palaeoecology, biomass, fecundity, Famennian, Anti-Atlas.

Merle Greif [merle.greif@pim.uzh.ch] and Christian Klug [chklug@pim.uzh.ch], Palaeontological Institute and Museum, University Zurich, Karl-Schmid-Strasse 4, 8006, Zurich, Switzerland.
James H. Nebelsick [nebelsick@uni-tuebingen.de], Department of Geoscience, Schnarrenbergstraße 94-96, 72076 Tübingen, Germany.

Received 13 August 2021, accepted 13 April 2022, available online 18 August 2022.

Introduction

Ammonoids, belonging to the extinct stem coleoids sensu Kröger et al. (2011), have become model organisms for several fields of palaeontological research such as biostratigraphy, biodiversity, biogeography and macroevolution (House and Senior 1981; Landman et al. 1996, 2013; Ritterbush et al. 2014; Klug et al. 2015a, b). Their species richness, conch characteristics, wide geographic distribution and long evolutionary history make them an especially important data source for such studies (Korn and Klug 2012). While diversity and disparity of fossil groups can be measured with certain methods to reduce biases, most researchers have refrained from estimating ammonoid abundances within a certain area and time. This is mainly due to the fact that the degree of faunal mixing (e.g., Andrews 2006), time averaging (Kidwell and Bosence 1991) as well as sediment accumulation rates (Wendt 1988 for the eastern Anti-Atlas) are difficult to estimate even for a defined area. The only reconstruction of an ammonoid mass occurrence thus far was carried out by Lukeneder et al. (2014) for an Early Triassic monospecific assemblage. This study dealt with the orientation of planispirally coiled ammonoids as well as 3D reconstructions of mass occurrences but no total ammonoid numbers were calculated.

Some places on the former Tafilalt and Maïder platforms are becoming increasingly famous as Fossillagerstätten (Frey et al. 2018, 2020; Klug and Pohle 2018; Frey 2019). Ammonoids and other pelagic fossils are found in mass occurrences ("Konzentrat-Lagerstätten" or concentration deposits sensu Seilacher 1970; Wendt et al. 1984; Pohle et al. 2020) at many localities, and are exceptionally well pre-

served in "Konservat Lagerstätten" (conservation deposits) at a few localities within the Tafilalt and Maïder (Frey et al. 2018). These characteristics make the region increasingly important and many studies concerning ammonoid stratigraphy, taxonomy, or other ammonoid related palaeontological topics in the eastern Anti-Atlas have been carried out within the last decades (Becker 1993, 1995; Belka et al. 1999; Korn 1999; Becker and House 2000a, b; Korn et al. 2000, 2014, 2015, 2016, 2018; Becker et al. 2002, 2018c; Klug and Pohle 2018).

According to their palaeogeographic position, the thickness of Devonian sediments varies laterally from the platform to the basin, especially in sediments of Late Devonian age (Hollard 1974; Toto et al. 2008). Mass occurrences of ammonoids such as those present within the former basin and platform areas (Fig. 1) are interesting for palaeontological and palaeoecological studies (Lukeneder et al. 2014). Such mass occurrences can be explained by different ecological factors such as rapid changes in sea level, climate, oxygen availability or salinity (Buggisch 1991). Under certain conditions, ammonoids flourished, which may have led to abundance peaks recorded in mass occurrences.

The reproductive rates of ammonoids, however, depended on body size, food availability and longevity (Korn and Klug 2007; De Baets et al. 2012; Laptikhovsky et al. 2012; Tajika et al. 2018, 2020). Reproductive rates and strategies of extinct ammonoids are difficult to assess due to the fact that, among others, their soft tissues are rarely preserved (Ritterbush et al. 2014; Pohle et al. 2020; Klug et al. 2021). Usually, statements concerning the reproductive rates of ammonoids can be made only by actualistic comparisons to recent cephalopods, which are known to have a wide range of reproductive strategies and life cycles (e.g., Lipinski 1998; De Baets et al. 2012; Mironenko and Rogov 2016; Pohle et al. 2020). In general, ammonoids and many other cephalopods (bactritids, orthocerids, early coleoids) had small embryonic conchs with a size of usually less than 2 mm. Accordingly, their eggs and hatchlings were small, although their size relative to the adults varied strongly and can be informative regarding fecundity (Korn and Klug 2007; De Baets et al. 2012; Laptikhovsky et al. 2012, 2017; Mironenko and Rogov 2016; Tajika et al. 2018; Pohle et al. 2020). Even though ammonoids are often compared to nautilids, it is widely accepted that ammonoids are more closely related to extant coleoids than to nautilids, which makes a direct comparison difficult (Jacobs and Landman 1993; Kröger et al. 2011; Korn and Klug 2012; Ritterbush et al. 2014; Fuchs et al. 2021).

This study addresses questions regarding the nature of the extremely high numbers of ammonoids found within some strata of Late Devonian age in the eastern Anti-Atlas and has the following aims:

– quantification of the approximate number of all preserved ammonoid specimens within some layers particularly rich in ammonoids in the study area by examining samples from different localities in the Tafilalt and Maïder. The obtained figures are used to extrapolate for a standardized rock volume and for one standard layer covering the whole study area;
– analyses of the size distribution of the sampled ammonoids allow testing whether juveniles and adults lived in the same region and whether the assemblage of the samples corresponds to the actual former association in number and age composition as reflected in conch sizes;
– estimating the biomass of all preserved ammonoids contained within the Famennian layers under consideration.

Fig. 1. Ammonoid mass occurrence (associated with brachiopods and orthocerids) from the lower Famennian of Madene El Mrakib, Morocco (prepared by Thomas Imhof, Trimbach); PIMUZ 37914.

Institutional abbreviations.—PIMUZ, Palaeontological Institute and Museum of the University of Zurich, Switzerland.

Geological setting

The Moroccan Anti-Atlas is chiefly a structural belt, appearing as a large anticlinorium oriented NE-SW (Kaufmann 1998; Robert-Charrue and Burkhard 2008). In this area, a remarkably complete sedimentary succession from the Precambrian to the late early Carboniferous in age is exceptionally well exposed, which shows one of the best documented biostratigraphic records of the Devonian Period worldwide (Wendt et al. 1984; Wendt 2021a,b). Devonian sediments crop out in a 1000 km long belt along the western and northern margin of the Tindouf Basin and reappear in more isolated E-W oriented synforms and antiforms in the Tafilalt and Maïder basins farther to the north-east (Wendt et al. 1984; Döring and Kazmierczak 2001; Frey et al. 2013).

During the Late Devonian, a platform and basin-topography formed along the northern margin of the Sahara Craton as a result of early Variscan tectonic movements and differential subsidence (Wendt et al. 1984). The area can be

Fig. 2. Geological map of the study area, the Tafilalt and Maïder, with indications of the localities and the approximate placing of the basins and platforms (map modified after Frey et al. 2020).

divided into the central, approximately N-S running pelagic Tafilalt Platform, the two flanking Maïder and Tafilalt basins in the west and east, as well as the Maïder Platform to the south-west (Wendt et al. 1984; Wendt 1985; Wendt and Belka 1991; Fig. 2). The two marine basins were connected via the shallower Tafilalt Platform (Wendt et al. 1984; Wendt 1985), which is the dominant Middle to Late Devonian geographic feature of the eastern Anti-Atlas (Wendt 2021a, b).

The Maïder Platform was exposed above sea-level during most of the Devonian and was submerged during the late Frasnian, partly only during the late Famennian (Wendt 1988). Late Devonian-aged deposits of the platform are discontinuous and locally reduced to only a few metres, while coeval deposits in the northern Maïder Basin can be up to 1200 m thick. These deposits consist of shale and some intercalated sandstone and limestone beds as the basin received muddy and finely clastic input from the surrounding, partly and temporarily emergent, pelagic platforms and from an eroded hinterland in the west (Wendt et al. 1984; Wendt 1988).

The adjacent Tafilalt Platform and Basin successions contain limestone layers of thicknesses that vary laterally (Wendt and Belka 1991). After the Frasnian/Famennian

boundary sedimentation break, early Famennian-aged cephalopod limestone was deposited on top of a karstified surface (Wendt et al. 1984; Wendt 1988). The Tafilalt Platform is characterized by condensed Upper Devonian, mainly grey and red cephalopod limestone, which passes laterally into shale with intercalated nodular limestone of the shallow Tafilalt Basin. Sedimentation took place on a gently sloping platform surface towards the north (Wendt et al. 1984; Wendt 1985, 1988). There, Famennian platform sediments may reach a thickness of 50 m but are often condensed to only a few metres in thickness with some hiatuses. Condensation is the strongest in cephalopod limestone, which was deposited in previously shallow or even emerged areas but generally decreases in the late Famennian-aged deposits (Wendt 1988). Successions of the marginal and southern Tafilalt Platform display a relatively continuous sedimentation that suggests permanent subtidal conditions (Wendt et al. 1984). Clastic input is nearly absent in the central and northern parts of the Platform but increases to the south with material deriving from older sediments further south. The sometimes quite highly diverse Famennian marine assemblages, comprising stenohaline elements such as echinoderms and cephalopods, indicates normal salinity with occasionally well-oxygenated bottom conditions and repeated anoxic phases (Wendt et al. 1984). The slopes had a mean angle of about 2°, which led to slumping and debris flows. The water depth probably did not exceed 500 metres and likely remained within the photic zone during the early late Famennian (Wendt 1988).

The south Tafilalt and Maïder regions comprise five structural domains with different structural axes (Baidder et al. 2016; Ait Daoud et al. 2019). Two different fold directions dominate the ductile deformation structures in the eastern Anti-Atlas (Tafilalt and Maïder). The first dominates the western part with an E-W axis and the second one dominates the eastern part with a NW-SE axis (Kaufmann 1998; Tawadros 2018; Ait Daoud et al. 2019). The main shortening stage responsible for the folding is the NE-SW late Variscan compression (Ait Daoud et al. 2019).

Material and methods

All material was collected in the Famennian successions of the Tafilalt and Maïder. Five limestone samples containing ammonoids in rock-forming numbers were taken at the following locations (Fig. 2):

Maïder, Madene El Mrakib (N30.73093°, W4.70749°): Large (50 to 150 mm thick, 0.5 to 1 m long), yellowish micritic limestone nodules (see Fig. 1) full of cephalopods and other fossils. The nodules are embedded in claystone with flat or limonitized fauna. PIMUZ 37914, 37915, 37922, 37923.

Tafilalt, Oued Ziz near Taouz (short Taouz; N30.92493°, W4.01920): light grey sparitic limestone layers, 50 to 100 mm thick with small subglobular ammonoids in rock-forming numbers in a sequence of beds with a similar facies. PIMUZ 37919, 37921.

Filon Douze 1 (N30.95809°, W4.04049°): Flat dark grey to yellowish nodules (50 to 100 mm thick, 100 to 500 mm wide), with abundant subglobular ammonoids. PIMUZ 37917.

Filon Douze 2 (N30.95805°, W4.04051°): Same as Filon Douze 1. PIMUZ 37918.

Oum El Jerane (N30.99353°, W4.13586°): Flat dark grey nodular limestone layers (50 to 100 mm thick), with abundant ammonoids including clymeniids and other fossils such as orthocerids, rugose corals, etc. PIMUZ 37916.

The samples were taken from large limestone nodules or nodular limestone beds, which were embedded in claystone, marl, and marly limestone. The sample weight varied between 1 kg and 2.7 kg with similar densities (SOM 1a, Supplementary Online Material available at http://app.pan.pl/SOM/app67-Greif_etal_SOM.pdf). The samples originate from the beds with the visually recognizable highest number of ammonoids.

All samples are stored at the Palaeontological Institute and Museum at the University of Zurich (PIMUZ 37914–37923).

Number of ammonoids and biomass.—Basic data: For the estimation of the numbers of all preserved ammonoids and their biomass within the study area, a series of values is needed: (i) the size of the estimated study area in the sedimentary basins prior to tectonic deformation; (ii) the absolute number and volume of ammonoid conchs within each sample. Further, the stratigraphic position of the samples (iii) was defined. To estimate annual ammonoid numbers and biomass, the time passed during deposition of 100 mm of sediment (iv) is needed and approximate sedimentation rates are estimated.

(i) The study area (Fig. 2) was folded tectonically between the Famennian and today, thus resulting in a reduced surface area of nowadays 11 094 km². To reconstruct the size of the area prior to folding around the time of sedimentation, different cross sections from within the area were used, which were published together with the corresponding geological maps (Alvaro et al. 2014; Benharref et al. 2014) and by Baidder et al. (2016). The length of one deformed bedding plane of each cross section was measured and put into relation to the actual surface length of the cross section. Thus, the degree of shortening could roughly be quantified. Measurements of one single bedding plane on the maps, unfortunately, does not provide very precise data. Measuring biases and the alignment of the measured transects (sections are not located in exact N-S or E-W direction) can also lead to errors. Despite these shortcomings, this method delivers an approximate value for the surface area before tectonic shortening.

In the NE-SW direction a transect through the Maïder and South Tafilalt Basin with a surface length of 105.5 km was chosen (Baidder et al. 2016). The length of one bedding plane along this transect is 110 km. Putting these lengths in relation leads to a tectonic shortening of 4.5 km or 4.27% in NE-SW direction. The surface length of another section oriented in SSW-NNE direction between Jebel El Atrous and Jebel El Mraïr (Alvaro et al. 2014) was measured to be 14 km long on the surface. A single bedding plane was measured to be 18.55 km, leading to a tectonic shortening

of 4.55 km (32.5%). The third cross section stretches from Jebel Mech Agrou to Jebel Bou M`ayz in NNW-SSE direction (Benharref et al. 2014). The section extends over 14.5 km; one bedding plane measures 17.1 km with a shortening of 2.6 km (17.93%). As an approximation, the mean percentage of tectonic shortening of the two last cross sections (25.2%) was taken as the shortening percentage for the N-S direction. The first shortening percentage after Baidder et al. (2016) was taken as an approximation for the shortening in E-W direction. Using these shortening percentages, the study area size (Fig. 2) prior to folding was estimated. Accordingly, the area (Fig. 2) covers 11,094 km² at present in its deformed state. If one folded layer was straightened out, it would measure about 15 512.5 km².

(ii) In order to determine the number and volume of ammonoid conchs in each of the samples, preparation of material was conducted using an air scribe. The weight of each sample was measured prior to preparation. Then, the entire limestone block was chipped away to separate the contained macrofossils. All macrofossils exceeding 1 mm in size were extracted and registered (SOM 2).

For an estimation of the volume of all ammonoids present within each sample, first the sample densities were needed. These were estimated using the water displacement method. A certain number of ammonoids of each sample was placed in water and the displaced volume was measured. The calculated densities vary between 2.62 g/cm³ and 2.85 g/cm³ and lie within, or very close to the normal density range of calcareous rocks (Carmichael 2017; SOM 1a). With the estimated densities, the volume of each sample prior to preparation and the volume of all prepared ammonoids within each sample was estimated by using the calculated densities and weight of each sample and the weight of all prepared ammonoids, respectively (V = m/d).

The total volume of ammonoids within each sample was determined by summarizing the measured volumes of prepared ammonoids (SOM 1a, b) and the computed volumes of destroyed ammonoids from the samples (SOM 3a, b). The volumes of ammonoids with diameters less than 5 mm were not reasonably measurable by water displacement, as the errors would have been too high. To calculate the volume of the mostly small ammonoids that were destroyed during preparation, the weight of random (concerning systematics) complete prepared ammonoids with different sizes was taken and the volume was calculated (V = m/d). The estimated volumes were plotted versus their diameter and a regression was made (SOM 3a, b).

(iii) The stratigraphic position of the samples was determined by identifying the species of the prepared ammonoids of each sample (Fig. 3) and by comparing these with index ammonoids (Becker 1993; Becker et al. 2002; Korn and Klug 2002; Korn et al. 2014, 2015, 2016, 2018; Becker et al. 2013; Hartenfels and Becker 2018). The samples from Madene El Mrakib and Taouz mainly contain specimens belonging to the species *Raymondiceras undulosum undulosum* and *Puncticeras lagowiense*. Additionally, the taxa *Armatites* sp. and *Cheiloceras subpartitum* were found (Fig. 3). After Becker (1993) and Becker et al. (2002), *Armatites planidorsatus*, *Armatites beatus*, and *Puncticeras lagowiense* occur in the *Praemeroceras petterae* Zone.

The samples Filon Douze 1 and Filon Douze 2 contained mainly specimens belonging to the species *Puncticeras lagowiense* and additionally specimens of the *Maeneceras* sp. were found. This sample was assigned to the middle Famennian *Maeneceras meriodinale* Zone sensu Korn and Klug (2015). This stratigraphic assignement is corroborated by the presence of *Maeneceras* sp. and *Acrimeroceras stella*, the latter missing in the examined samples but one specimen was found in these strata some tens of meters further (Fig. 3; Becker 1993; Klug 1997; Becker et al. 2002).

The sample from Oum El Jerane shows a higher ammonoid diversity. Specimens of *Kosmoclymenia* sp. were found together with *Erfoudites rherisensis*, *Discoclymenia pola*, *Costoclymenia ornata*, and *Prionoceras jeranense* (taxon lists: Korn et al. 2000, 2014, 2015, 2016, 2018; Becker et al. 2013). This sample was stratigraphically assigned to the Famennian *Costaclymenia muensteri* Zone (Fig. 3; Becker et al. 2002, 2013; Hartenfels and Becker 2018).

(iv) Approximate sediment accumulation rates and the time that is contained within the defined 100 mm of layer thickness can only be estimated. Sedimentation is usually not continuous and depositional gaps as well as changing sediment accumulation rates are the norm depending on various environmental factors. Here, preservation rates rather than true sediment accumulation rates are estimated (Strasser 2016). Following Wendt and Aigner (1985), we assume a Bubnoff unit between 1 and 5 (1–5 m/myr), as minimum sedimentation rate for cephalopod limestone which corresponds roughly to the suggestions of Wendt (1988).

Calculation of the total number of ammonoids and their biomass.—The estimated number of ammonoids that may be preserved per layer thickness in the study area was calculated by using the values explained above. The number of ammonoids per 1 kg within each sample were multiplied with the number of times a 1 kg sample (367 cm^3) fits in the volume of the layers under consideration in the area (Table 1). Pre-Variscan tectonic movements caused increasing movements in the eastern Anti-Atlas during the Late Devonian (Wendt 1985, 1988, 2021b; Baidder et al. 2016) with small-scale horst and graben-structures, in turn linked with very local hiatuses and rapid changes in thickness. Hence, an accurate spatial reconstruction of distinct strata is impossible in the absence of intense mapping, logging of sections and detailed seismic profiles. Consequently, we rely on standardized volumes and sediment accumulation rates.

For the volumes, we set the standard thickness to 100 mm and for the area, we use a minimum value of 1 km^2 and the approximate surface of the Maïder and Tafilalt basins as outlined above as maximum value. For the sedimentation rates, a value of 5 mm per 1000 years is used, which was taken from the literature based on facies (Strasser 2016) and earlier estimates (Wendt 1988: fig. 13). For simplicity, it is

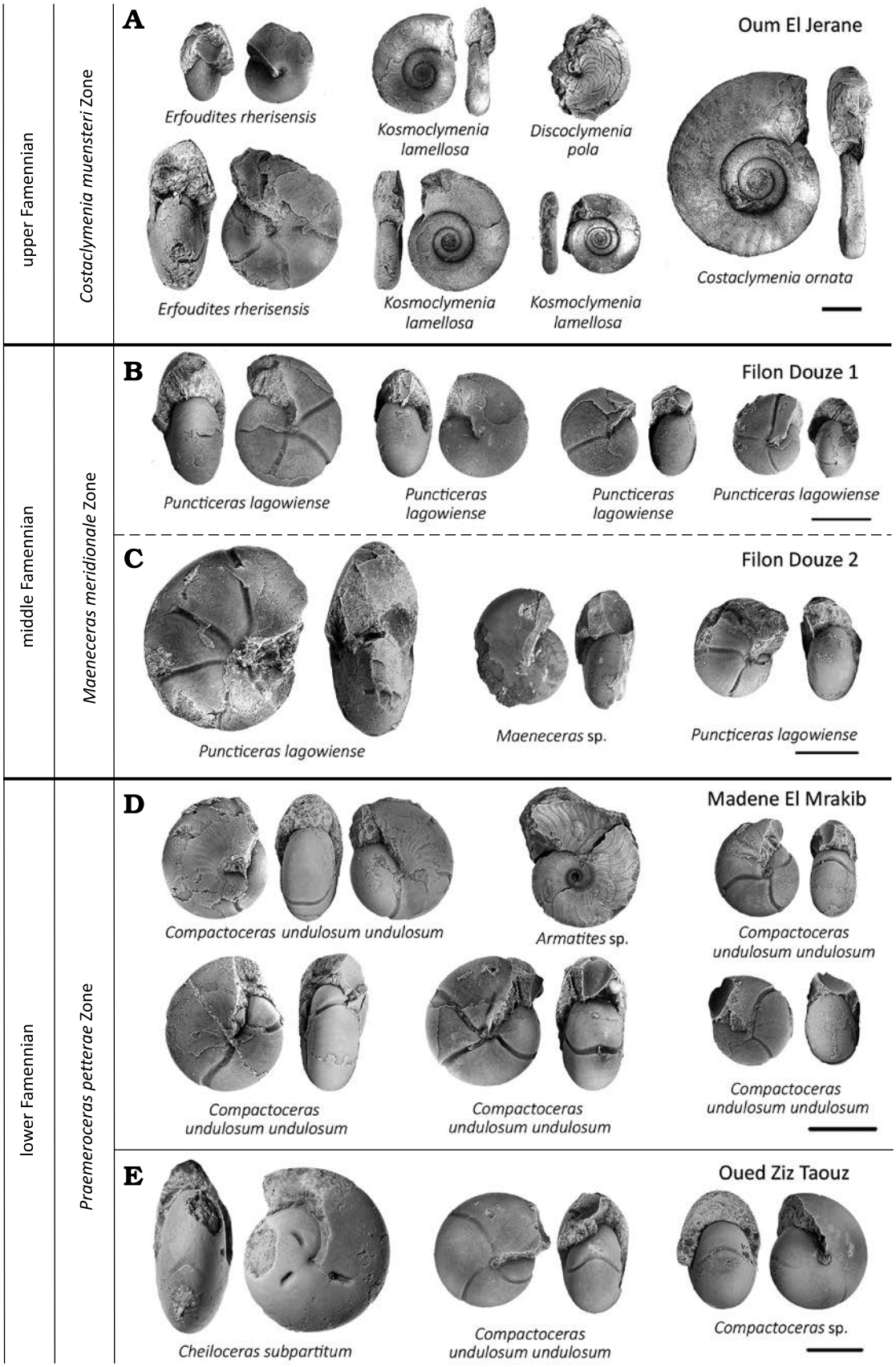

Fig. 3. Typical ammonoids from lower, middle, and upper Famennian, Anti-Atlas, Morocco. **A**. Sample PIMUZ 37916, Oum El Jerane. **B**. Sample PIMUZ 37917. **C**. Sample PIMUZ 37918. **D**. Sample PIMUZ 37915. **E**. Sample PIMUZ 37919. In order to show various aspects of variation, we sometimes display more than one specimen per species. Scale bars 10 mm.

Table 1. List of all equations and the estimated ammonoid number and biomass exemplary with the data from the sample Taouz. The biomass was calculated by using the average density of seawater (1.025g/cm³). The numbers with data from all other sample were calculated following the same method as in Taouz.

Variable and unit	Abbreviation and equation	Result for Taouz sample
Layer thickness (km)		0.0001
Layer volume within whole outcrop area (km³)	V = area × layer thickness	1.55125
Volume for the area of 1 km² (km³)	V 1 km = 1 km² × layer thickness	0.0001
Volume for 1 kg of the sample (km³)	V 1 kg	3.67E-13
Number of ammonoids per kg in the sample	Nb1T	91
Estimated weight of the layer in whole area (kg)	WA = V/V 1 kg	4.23E+12
Estimated weight of the layer in the area for 1 km² (kg)	WA 1km = V 1 km/V 1 kg	2.72E+08
Number of ammonoids	An = WA × Nb1T	3.83E+14
Number of ammonoids in the area of 1 km²	An 1 km = WA 1 km * Nb1T	2.47E+10
Ammonoid total volume (cm³)	AVTT	296.62
Ammonoid body chamber volume (cm³)	AVCT	68.64
Ammonoid biomass in sample (g)	AB = AVTT × 1.025 g/cm³	304.04
Ammonoid chamber mass (g)	ABC = AVCT × 1.025 g/cm³	70.36
Biomass per 1 kg of the sample weight (g)	B 1 kg = AB/sample weight (kg)	141.41
Body chamber mass per 1 kg of the sample weight (g)	BC 1 kg = ABC/sample weight (kg)	32.72455
Biomass within the whole outcrop area (kg)	BM = (B 1 kg × WA)/1000	5.98E+14
Body chamber mass within the outcrop whole area (kg)	BMC = (BC 1 kg × WA)/1000	1.38E+14

assumed that the mass accumulations of the samples from the *Praemeroceras petterae* Zone extend over the whole study area, as similar accumulations can be found at many localities (here, differences in thickness, sediment accumulation rates, etc. are ignored). For the younger samples we do not know the geographical extend of the layers they originate from. Based on the simplifying assumption of a homogeneous distribution over a large area, the numbers of preserved ammonoids as well as their palaeo-biomass for the whole study area and for an area of 1 km^2 with a layer thickness of 100 mm are calculated.

The biomass (living mass; here: the total mass of the organism) of all preserved ammonoids as far as they were recorded in the respective sediment within the former basins was calculated by multiplying the volume of all ammonoids for each sample with the density of sea water (~1025 kg/m³, Table 1), as it is assumed that they were nearly neutrally or only slightly negatively buoyant (Lemanis et al. 2015; Tajika et al. 2015; Naglik et al. 2016; Yacobucci 2018). Furthermore, the biomass volume per 1 kg sample was multiplied with the number of times the 1 kg sample fits in the volume of the layers in the study area and for a standard area of 1 km^2. This calculation comprises all parts of the ammonoid including the shell with the gas-filled phragmocone.

A second biomass estimation of only the soft tissue mass was accomplished by multiplying the body chamber volume with sea water density. It is assumed, that the total individual mass of an ammonoid is the sum of all parts of the ammonoid (not only that of the soft tissues). Accordingly, the biomass we use equals the total mass of the living ammonoids within the study area (or 1 km^2) and the layer thickness standardized to 100 mm, in all aggregation states (Llopis-Belenguer et al. 2018) as far as they are preserved in our samples.

Results

Total ammonoid number and biomass.—Preparation of the samples yielded a total amount of 1393 more or less complete ammonoid specimens with diameters between 2.5 and 50.0 mm in all samples together. 1085 mostly small ammonoids with diameters between 1.0 and 18 mm were destroyed during preparation, but their diameters were noted (SOM 2). The volume occupied by the extracted ammonoids ranges between 33% of the rock volume in the sample from Filon Douze 2 and 57% in the Filon Douze 1 sample (Fig. 4). The theoretical volume of destroyed ammonoids was determined using a power function (SOM 3a, b) and occupies between 1 and 3% of the total ammonoid volume, therefore deviations due to measuring errors are negligible.

The total ammonoid volume is only slightly larger than the volume of the prepared ammonoids; the lowest ammonoid per rock percentage is found in the sample Filon Douze 2 with 34% (opposed to 33% without the destroyed specimens). The highest percentage is found in the sample Filon Douze 1 with 58% (opposed to 57%) of the sample consisting of ammonoids (Fig. 4). The corresponding numbers of specimens per 1 kg of limestone (about 367 cm³) were calculated for all locations. At Filon Douze 2, 1 kg of limestone contains 156 ammonoids and in Filon Douze 2, 1 kg of limestone contains 185 ammonoids. The highest number of ammonoids is found in the sample from Madene, though, with a number of 459 ammonoids, many of them with very small diameters.

Estimates of the total number and biomass of preserved ammonoids.—The values mentioned above were used to calculate the total as well as the annual ammonoid number within the standard study area of 1 km^2 and the entire

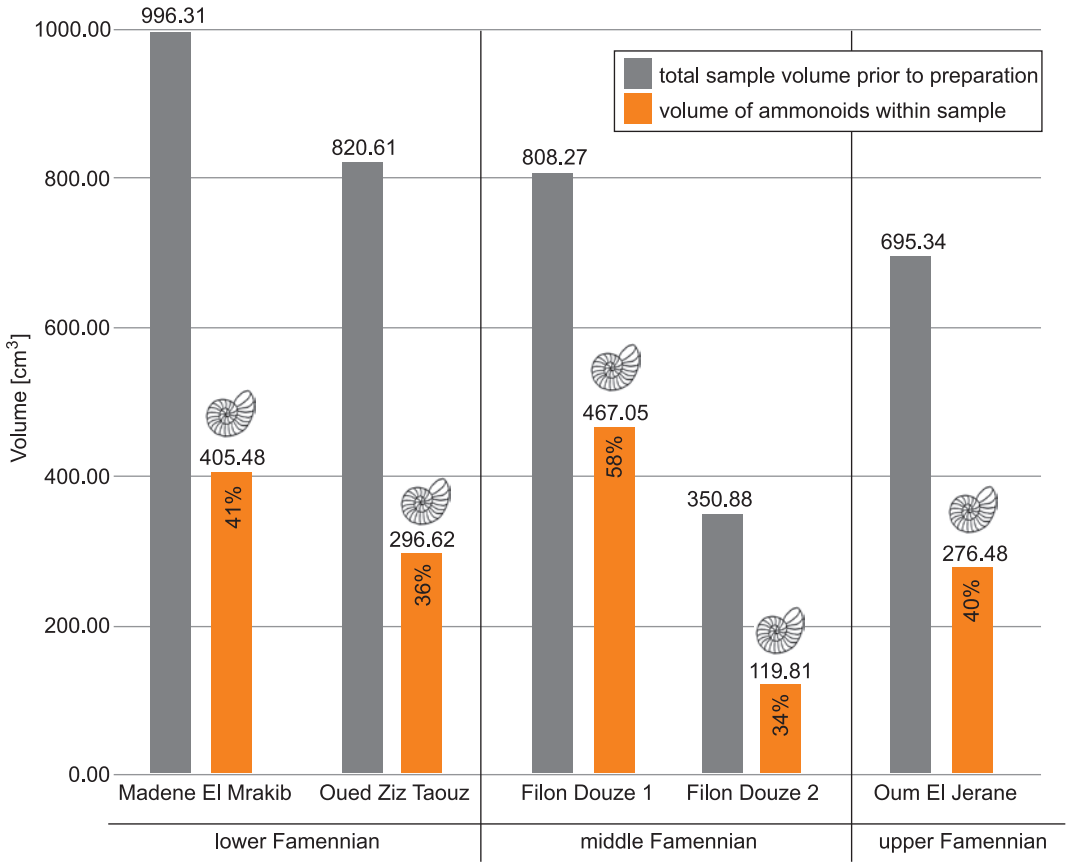

Fig. 4. Total volume of each sample and the volume of all ammonoids in the respective samples; including complete ammonoids and small ammonoids destroyed during preparation.

Table 2. Total number of ammonoids in the whole study area and for an area of 1 km^2 with the data from every sample and the estimated number of ammonoids that were preserved within one year of time. Both with a layer thickness of 100 mm. The numbers were calculated as shown in Table 1.

Sample name	Weight of the sample (g)	Total number of ammonoids	Number of ammonoids		Quantity per 1 km²	Annual number of ammonoids	
			within 1kg sample weight (367 cm³)	within the whole study area (15512.5 km²)		for the whole area	per 1 km²
Madene	2700	1240	459	1.94E+15	1.25E+11	9.71E+10	6.26E+06
Taouz	2150	195	91	3.83E+14	2.47E+10	1.92E+10	1.24E+06
Filon Douze 1	2150	398	185	7.82E+14	5.04E+10	3.91E+10	2.52E+06
Filon Douze 2	1000	156	156	6.59E+14	4.25E+10	3.30E+10	2.13E+06
Jerane	1940	142	73	3.09E+14	1.99E+10	1.54E+10	9.95E+05

Table 3. Total biomass and annual biomass estimates with the data from every sample for the whole study area and for an area of 1 km^2. Both with a layer thickness of 100 mm. The values for annual biomass were estimated by division by 19 418 (estimated time contained within the 100 mm layer thickness).

Sample name	Ammonoid total volume per sample (cm³)	Ammonoid biomass (g)	Weight of the sample weight (g)	Ammonoid biomass			Annual number of ammonoids biomass (t)	
				per 1 kg of the sample (g)	for the whole area (t)	per 1 km² (t)	for the total outcrop area	for 1 km²
Madene	405	416	2700	154	6.51E+08	41943.8	32532.6	2.10
Taouz	297	304	2150	141	5.98E+08	38531.8	29886.2	1.93
Filon Douze 1	467	479	2150	223	9.41E+08	60670.7	47057.7	3.03
Filon Douze 2	120	123	1000	123	5.19E+08	33461.8	25953.8	1.67
Jerane	276	283	1940	146	6.17E+08	39803.8	30872.8	1.99

Maïder plus Tafilalt area of 15 512.5 km^2, respectively, using a standard sediment thickness of 100 mm. For the standardized area of 1 km^2, the estimated ammonoid numbers range from 19.9×10^9 to 12.5×10^{10} ammonoids (Table 2). The according biomass estimates range between 33 462 t and 60 671 t (Table 3). For the entire study area, the estimated

Table 4. Body chamber (bio-) mass estimates with the data from every sample for the whole study area and for an area of 1 km^2. Both with a layer thickness of 100 mm. The values for annual biomass were estimated by division by 19 418 (estimated time contained within the 100 mm layer thickness).

Sample name	Body chamber volume per sample (cm^3)	Ammonoid biomass (g)	Weight of the sample (g)	Ammonoid biomass			Annual number of ammonoids biomass	
				per 1 kg sample (g)	per sample within the whole area (t)	per 1 km^2 (t)	for the total area (t)	for 1 km^2 (t)
Madene	234	240	2700	89	3.75E+08	2.42E+04	18753.1	1.21
Taouz	104	107	2150	50	2.11E+08	1.36E+04	10528.9	0.68
Filon Douze 1	87	89	2150	42	1.75E+08	1.13E+04	8774.8	0.57
Filon Douze 2	37	38	1000	38	1.60E+08	1.03E+04	8003.6	0.52
Jerane	125	128	1940	66	2.80E+08	1.80E+04	13980.6	0.90

ammonoid numbers vary between 30.9×10^{13} and 19.4×10^{14} ammonoids (Table 2). The biomass ranges from 51.9×10^{7} t to 94.1×10^{7} (Table 3).

Estimates of the annual number of preserved Famennian ammonoids and biomass.—To estimate the numbers of ammonoid conchs that accumulated within one year and the theoretic biomass, the time contained within the 100 mm of sediment needed to be known.

Assuming a sediment accumulation rate of 5 mm per 1000 years, a time of 20 000 years is estimated. With that value, the annual conch accumulations within an area of 1 km^2 is estimated to range from 99.5×10^{4} to 62.6×10^{5} (Table 2). The annual ammonoid conch accumulation within the whole study area is estimated to range from 15.4×10^{9} to 97.1×10^{9} (Table 2). For an area of 1 km^2 the annual biomass estimates range from 1.67 t to 3.03 t (Table 3). The annual biomass estimated for the whole area range from 25 954 t to 47 058 t (Table 3).

For the soft tissue only-biomass of all preserved ammonoids in the study area, the body chamber volume was needed as mainly this part of the ammonoid shell was filled with soft tissue. Since the most common ammonoids found in the early Famennian-aged samples belong to the cheiloceratids, these were used for body chamber volume calculations and the results used as approximation for all specimens. A cheiloceratid such as *Compactoceras undulosum undulosum* (Fig. 3), with the largest diameter of 32.5 mm found in the samples, has a total shell volume of 5.8 cm^3 (SOM 3b). The diameter of this ammonoid minus the body chamber is 24.8 mm (Fig. 5B). By subtracting the volume of an ammonoid with a diameter of 24.8 mm from the whole volume of a 32.5 mm sized ammonoid (5.84–2.86 cm^3), a body chamber volume of 2.98 cm^3 is obtained (51% of the whole ammonoid). The soft tissue mass per sample was calculated by estimating the body chamber volume of each counted ammonoid within the sample using the estimated volumes (SOM 4). This approach does not regard soft tissues that might have been outside of the ammonoid shell. Similarly, water contained in the mantle cavity is included.

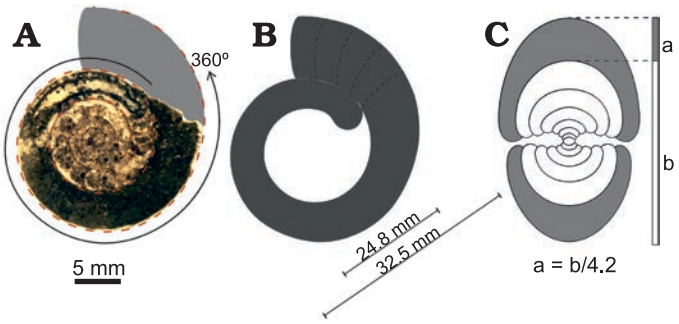

Fig. 5. A scheme of shell measurements in *Cheiloceras* sp. from the lower Famennian of Madene El Mrakib, Anti-Atlas, Morocco (PIMUZ 37923). **A**. Polished sagittal section with the possible continuation of the ammonoid shown in grey. The photographed specimen is incomplete, parts of the body chamber are missing, and the specimen was probably larger as suggested by the reconstructed area. **B**. The body chamber shown without phragmocone; dashed lines indicate possible positions of the terminal aperture of the ammonoid. The diameter of the largest complete ammonoid from Madene sample and the diameter of the specimen without the body chamber are shown. **C**. The cross section showing the way the aperture opening was calculated. The number 4.2 is an average value from measurements of different sized specimens; a, apertural height; b, diameter of previous demi-whorl; conch diameter = a + b.

Table 5. Logarithmic size classes of ammonoid conch diameters.

Size class	Logarithmic diameter	Maximum diameter
1	0.1	1.26
2	0.2	1.58
3	0.3	2.00
4	0.4	2.51
5	0.5	3.16
6	0.6	3.98
7	0.7	5.01
8	0.8	6.31
9	0.9	7.94
10	1	10.00
11	1.1	12.59
12	1.2	15.85
13	1.3	19.95
14	1.4	25.12
15	1.5	31.62
16	1.6	39.81
17	1.7	50.12
18	1.8	63.10
19	1.9	79.43
20	2	100.00

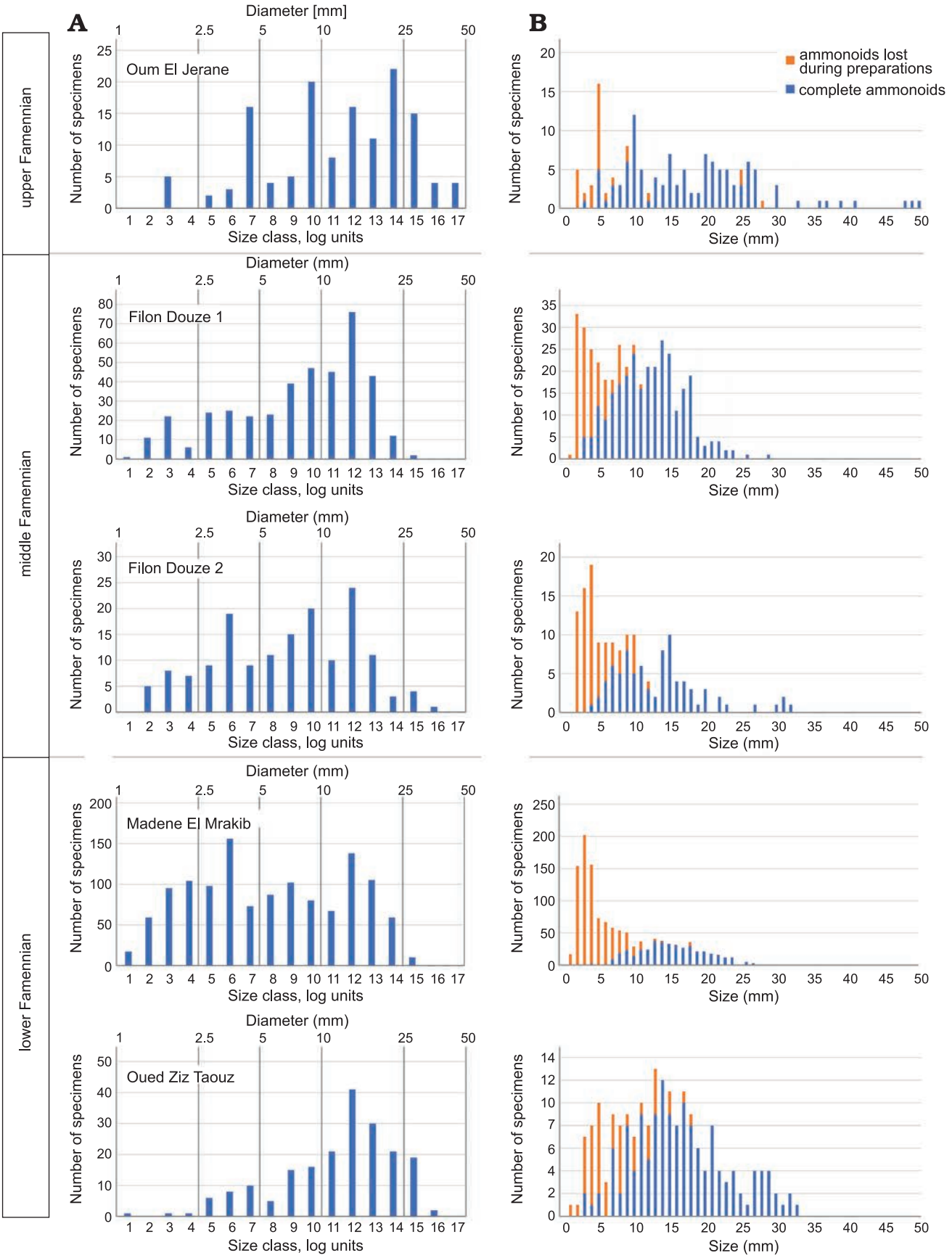

Fig. 6. Size distribution of all ammonoids in each sample. **A**. Number od specimens (without specimens lost in preparation) vs. size class. The size classes 1–20 were defined by using the logarithm of the log diameters shown in Table 5. **B**. The ammonoids counts plotted on a metric axis.

The body chamber mass, as proxy for the biomass of only the soft tissues, is estimated to range between 8003 t and 18 753 t per year within the whole study area (Table 4). For the area of 1 km^2 the body chamber mass is estimated to range between 520 kg and 1210 kg per year (Table 4).

Size distribution of the sampled ammonoids.—Ammonoid conch sizes were plotted ordered in metric size classes. These show a decrease in number from smaller to larger specimens in all samples (Fig. 6). However, owing to the fact that ammonoid conchs grew logarithmically, a second plot for the size distribution using logarithmic size classes was made for all samples (Fig. 6). We used the log size classes defined by Walton et al. (2010) to plot the conch diameter data (Table 5). In all five log plots, a peak in abundance is visible for conch sizes of about 16 mm (size class 12, Fig. 6). The abundance decreases rapidly after this peak. Furthermore, an abundance peak of small conchs can be seen in the sample of Madene El Mrakib for sizes of about 4 mm (size class 6, Fig. 6). Generally, the abundance of small ammonoids is remarkably high in the Madene El Mrakib sample. A very similar pattern can be seen in the sample of Filon Douze 2 and is also assumed for the sample Filon Douze 1. In the sample of Taouz, a much lower abundance of small ammonoids was recorded while the Oum El Jerane sample shows several abundance peaks (probably owing to the diversity and disparity in morphology as well as adult size of the contained ammonoids).

Discussion

Number of ammonoids

The number of preserved ammonoids versus the number of living ammonoids—error estimation.—The estimated total number of preserved ammonoids from the various Famennian layers and their biomass gives an impression of the order of magnitude of the preserved number of co-occurring ammonoids, but several uncertainties and biases remain. Many of the needed values cannot be measured exactly and estimates had to be made. Counting mistakes might have led to errors as well.

In the samples from the Tafilalt and Maïder, all ontogenetic stages are represented (Fig. 6) from hatchlings via juveniles to adult specimens. Given the small size of the hatchlings of ca. 1 mm, it appears likely that the true number of small ammonoids might have been even higher. During preparation, these very small specimens can easily be overlooked and were not counted in such cases.

Nevertheless, the estimated numbers are used as reference points for the number of ammonoids that were preserved in the study area (1 km^2 respectively). But how is this number related to the number of ammonoids that indeed lived during that time interval? The estimated number of fossilized ammonoids within a certain area and time can only give a hint to how many ammonoids have actually lived (a minimum value, due to incomplete fossil preservation) and do not lead to fully representative numbers for the former association. Unknown variables like the fossilisation rate and the degree of incompleteness of the fossil record make it extremely difficult to calculate total fossil numbers accurately (Marshall et al. 2021). Due to loss caused by non-fossilisation, the estimated number of 30.9×10^{13} to 19.4×10^{14} preserved ammonoids within the whole study area is likely to be lower than the actual number of living ammonoids during that interval. The ammonoid number and biomass estimates are meant to serve as an indication and as a reference point for comparable attempts. Another factor that can alter the number of ammonoids is dissolution and differential diagenesis, which may have dissolved ammonoids in limestone-marl alternations (Ricken 1985; Ricken and Eder 1991; Munnecke and Westphal 2005).

Furthermore, several other important factors can lead to differences between the number of fossilized ammonoids and the number of formerly living ammonoids. The estimates were made with samples that were taken in places of ammonoid mass occurrences that can be found all over the Tafilalt and Maïder (Fig. 7). Other localities and strata in the area show a much lower abundance of ammonoids. The laterally varying fossil abundance within the study area as well as taphonomic factors including sorting and winnowing before sedimentation or recrystallisation after burial may alter the ammonoid numbers significantly. Projections made with counts from samples taken from ammonoid mass occurrences might therefore also lead to overestimations for the whole area and that is why the number for only 1 km^2 were made as well.

We cannot know all processes that influenced the completeness of these taphocoenoses. Nevertheless, in order to get a better idea of the missing specimens, we plotted the sums of preserved and crushed specimens from Madene El Mrakib and projected exponential and logarithmic trend lines through the data points (Fig. 8). These trendlines already provide an impression of how many specimens might be missing with sizes of less than 4 mm, which has the highest specimen count. When projecting the trendlines through the 4 mm-data point, we obtain a field in these bivariate plots, which might come close to the missing specimens. In any case, it is likely that the values calculated here are still far below the actual numbers.

Possible reasons for mass occurrences.—One possible explanation for mass occurrences is catastrophic mass mortality, which can be caused by several processes. A basic requirement is, of course, that a high number of individuals lived together in space and time. In many localities and strata, a high benthic diversity can be found in the Tafilalt and Maïder and well oxygenated water conditions are suggested within the water column during much of the Devonian (Becker et al. 2018b; Frey et al. 2018) but the accompanying fauna within the samples is not very diverse. Mainly coiled ammonoids were found together with some orthocones and

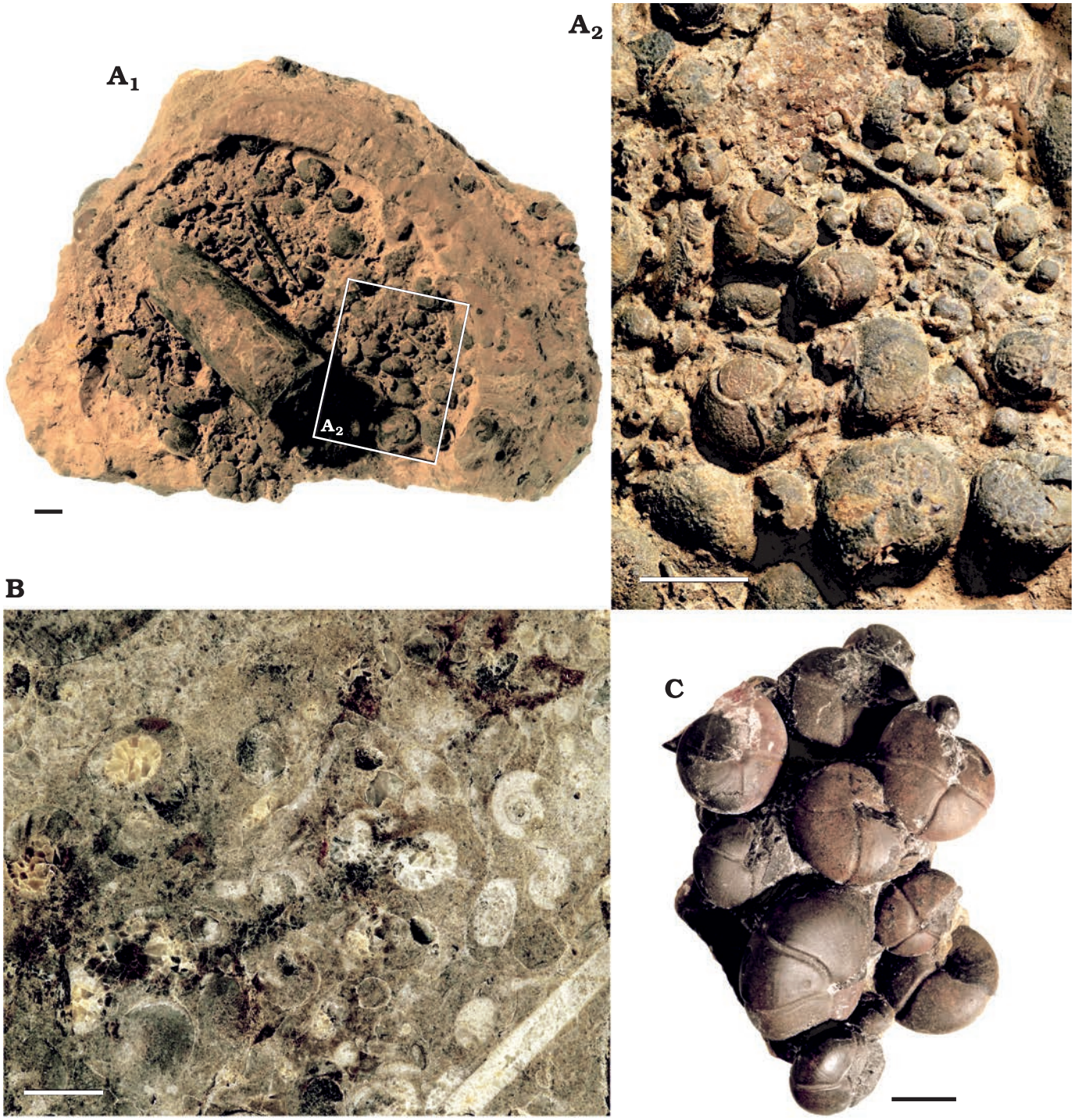

Fig. 7. Ammonoid mass occurences from the different localities in the Anti Atlas ôf Morocco. **A**. PIMUZ 37920, concretion showing a ammonoid mass occurence and an orthocone (A_1) with close up (A_2) from Achguig, north east Tafilalt, lower Famennian. **B**. PIMUZ 37921, polished section of an ammonoid mass occurrence from Taouz, Tafilalt, lower Famennian. **C**. PIMUZ 37922, prepared ammonoids from an association from Madene EL Mrakib, Maider, lower Famennian. Scale bars 10 mm.

rarely some brachiopods (most at Filon Douze 2). Perhaps, ammonoid blooms due to favourable conditions, or seasonal mass aggregations for reproduction, followed by mass mortality due to semelparity, have led to high numbers of ammonoids living or dying at the same time and region (Doubleday et al. 2016; Hoving et al. 2017). Phases of lethal anoxic conditions could have repeatedly occurred between times with more or less normal conditions, leading to the high numbers of individuals dying and becoming fossilised later on. Especially the Late Devonian was repeatedly affected by reduced oxygen conditions (Buggisch 1991; Wendt and Belka 1991). Abiotic events such as anoxia, algal blooms, mass dying of primary producers etc. may have caused the sudden death of marine animals as well

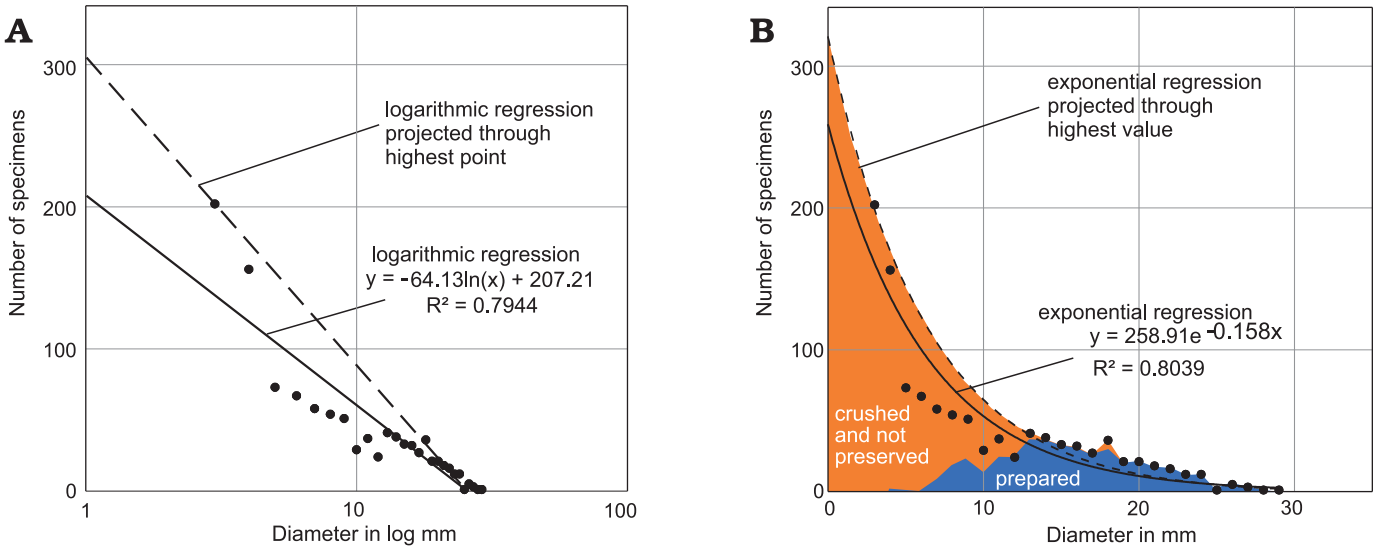

Fig. 8. Estimating the number of missing specimens from Madene El Mrakib. **A**. Diameter plotted in log; the dashed line demarcates the possibly missing data based on the highest count at a diameter of 4 mm. **B**. Diameter plotted linearly; prepared specimens are marked by the blue field; the black dots mark the sums of prepared and crushed specimens; the orange field adds those specimens, which we might have missed entirely, either because of non-preservation or because they were overlooked during preparation; this is based on the regression line that was moved to the highest point of small specimens.

and result in a frozen image of the current faunal situation (including census communities). The analysed samples do not show indications for such events, except for low oxygen (low diversity of benthos, rich in pyrite and organic matter). Instead, the samples contained mainly coiled ammonoids in most post-embryonic ontogenetic stages, supporting the possibility of a sudden mass mortality (Doyle and Macdonald 1993; Yacobucci 2018).

Condensation by low sediment accumulation rates or winnowing is common in the Devonian layers of the eastern Anti-Atlas, particularly in the platform areas, and can also lead to a high fossil abundance (Wendt et al. 1984; Lukeneder et al. 2014; Pohle et al. 2020). This may also cause time averaging and faunal mixing (Kidwell and Bosence 1991), thereby providing an alternative explanation for the joint presence of different life stages.

Further, post mortem transport and sorting can result in mass occurrences. We did not find indications for sorting in most samples, since quite a range of conch sizes is present and combined with fossils with a different composition as well as an often micritic matrix. Additionally, more abraded or broken conchs could be expected, which is not common in our samples (Fig. 1).

Also, the time needed for a cephalopod to become waterlogged, sink and become embedded has been debated (Chamberlain et al. 1981; Chirat 2000; Wani et al. 2005; Yacobucci 2018). For example, for the extant nautiloid *Nautilus pompilius,* a rather long drift of the empty shells was reported (Chirat 2000; Yacobucci 2018), while Yacobucci (2018) suggested a relatively short drifting distance for cephalopods otherwise, *N. pompilius* being the exception. Yet, fossil cephalopod conchs with diameters of less than 50 mm, like the ones studied here, are thought to have sunk relatively soon after death as water floods the phragmocone through the siphuncular tube (Wani et al. 2005; Yacobucci 2018). Long distance post mortem transport appears unlikely for the widespread high ammonoid abundance in the Tafilalt and Maïder also because these basins were surrounded by shallow water or land on three sides (Fig. 2). Other processes that may lead to mass mortalities and thus mass accumulations of conchs are strong changes in salinity, drastic sea level-changes, algal blooms producing toxins, etc.

Comparison to modern coleoids.—Comparison of ammonoid numbers and biomass to that of modern coleoids can provide some guidelines to the accuracy of the estimates presented herein. Such a comparison is justified because of the shared ancestry of the two groups (Kröger et al. 2011; Klug et al. 2015b), similar habitats and their overlapping reproductive rates (De Baets et al. 2012, 2015; Tajika et al. 2018). Nigmatullin (2004) estimated the annual biomass of ommastrephid squids to be on average 400 million tons within all world's oceans (surface area of 361 900 000 km^2). Assuming an even distribution of these squids within the oceans, this would lead to an ommastrephid biomass of ~17 146 t within an area of the size of the study area in the Anti-Atlas. The estimated Devonian biomass of all preserved ammonoids is higher per area but within the same order of magnitude (between 25 954 and 47 058 t). This comparison is problematic as the estimated numbers in this study originate from samples taken in layers of ammonoid mass occurrences, where the exact processes explaining this cannot be fully quantified. This is certainly not the case for the estimates of the ommastrephid squid biomass, which are based on the assumption of an even distribution of these cephalopods in the world's oceans. The similar order of magnitude of the fossil occurrences discussed here and the recent squids points at the possibility that the order of magnitude we found for the Famennian ammonoids is plausible or a low estimate.

Size distribution and reproductive strategies

Reproductive strategies and egg number.—The ammonoid counts show a significantly higher absolute number of small ammonoids in comparison to large ones: In Madene, 69.4% have a conch diameter of less than 10 mm and this value is probably quite underestimated (Fig. 6). This distribution is not surprising as ammonoids are assumed to be r-strategists (type III survivorship curves; Lloyd 1978) and therefore produce a large number of offspring with a high mortality and a very low percentage reaching maturity (Korn and Klug 2007; Walton et al. 2010; De Baets et al. 2012; Laptikhovsky et al. 2012; Ritterbush et al. 2014; Tajika et al. 2018). The samples show the expected distribution pattern for r-strategists with a type III-survivorship as expected in general for ammonoids.

The bivariate plot displays the diameter logarithmically owing to the growth mode of ammonoid conchs (cf. Walton et al. 2010). Two maxima can be seen at three of the plots at the size classes 6 and 12 (Fig. 6). The peak at size class 6 is not visible in the samples Oum El Jerane and Taouz (Fig. 6). One possible explanation is the coarse recrystallisation of the ammonoids from Taouz. The crystal size in the sparitic matrix of this sample exceeded the size of the smallest specimens found in the other samples. Alternatively, this size class might have been transported away by winnowing. Another factor that contributed to these differences between samples is the different stratigraphic origin of the samples. Rounding of measurements and assignment of specimens to the size classes may also have caused minor deviations.

Possibly, the two distinct maxima were caused by iteroparity (Laptikhovsky et al. 2013); a reproductive strategy of cephalopods that spawn more than once a year (e.g., Rodrigues et al. 2011) could lead to two such maxima. However, many coleoid cephalopods and ammonoids are semelparous (Rocha et al. 2001). Consequently, the presence of several size maxima is most likely linked with the presence of more than one species.

But what led to the extremely high numbers of ammonoids that are found in many Devonian strata of the eastern Anti-Atlas? Favourable environmental conditions (food availability, oxygenation, etc.) are key factors required for cephalopod mass occurrences. This is somewhat corroborated by the shared great abundance of conodonts, brachiopods, orthocerids and also microvertebrates in the same strata and regions. Although superficially, the Famennian samples seem to be of low diversity, this impression might be wrong, when the entire diversity including microfossils is taken into account (e.g., Belka et al. 1999) and when the sample is big enough.

The reproductive rates of cheiloceratids and other small globose ammonoids of the Famennian likely also play an important role. Tajika et al. (2018) estimated the egg numbers for some large Cretaceous ammonites to have reached possibly up to several millions per female. Boyle (1983) estimated egg numbers for modern coleoids with ca. 700 000 eggs in *Octopus cyanea* and ca. 650 000 eggs in *Dosidicus gigas*. In order to estimate the number of offspring of the relatively small cheiloceratids, the body chamber volume and the hatchling volume are needed (Korn and Klug 2007; De Baets et al. 2012; Mironenko and Rogov 2016). Measurements of the sampled cheiloceratids indicate a quite long body chamber of at least 360°, which had rather low whorl cross section (Fig. 5). Unfortunately, no unequivocally complete adult cheiloceratids were found in the early Famennian-aged samples and therefore, the exact length of the body chamber of these cheiloceratids cannot be measured (Fig. 5A). Nevertheless, whorl expansion rate and body chamber length roughly correlate in ammonoids (Okamoto 1996; Klug 2001). The whorl expansion rate of cheiloceratids is usually below 2.0 and hence, the length of their body chambers was around 360° or even longer. Accordingly, we assumed 360° for the following discussion for simplicity.

Presuming that 8% of the body chamber of an adult female ammonoid was filled with gonads (De Baets et al. 2012), a cheiloceratid of 32.5 mm diameter and with a body chamber volume of ca. 2980 mm^3 (Fig. 5; SOM 4) has an estimated gonad volume of ca. 231 mm^3. One egg occupied an average of at least 1 mm^3, which corresponds to the size of the smallest ammonoids in the samples (De Baets et al. 2015: table 5.1) leading to a ca. 230 eggs per adult female assuming semelparity. This reproductive rate is at the lower end of ammonoid fecundity, but accords well to the small adult conch size (De Baets et al. 2012; Mironenko and Rogov 2016; Tajika et al. 2018). Of course, only very few of the offspring of one female reached adulthood but the size distribution with an increase in abundance with decreasing conch diameter (Fig. 6) can easily be explained with only few adults producing a moderately large number of hatchlings. In order to explain the mass occurrences and size-distributions therein, spawning events may explain the abundance peaks (Rocha et al. 2001; Nigmatullin and Markaida 2009; Laptikhovsky et al. 2013; Vijai et al. 2014). Of course, other phenomenons such as a short duration from hatching to reproduction might have also contributed to the high specimen numbers.

Size distribution and ecology.—Most size classes from hatchlings to adults are found together in all samples but one (hatchlings and early juveniles are unusually rare in the sample from Taouz). Hence, no geographic separation of juvenile and adult ontogenetic stages is evident. A geographic separation could be the result of migration patterns in conjunction with spawning events that can be observed in some Recent cephalopods (Ritterbush et al. 2014). As reported by Ikeda and Wani (2012), however, life modes of different suborders of Cretaceous ammonoids were a lot more diverse than in modern nautilids. The absence of a geographic separation suggests that the early Famennian ammonoids of the Tafilalt and Maïder under consideration did not migrate extensively during their life and all developmental stages lived in the same region. It is not known, however, whether or not a vertical niche partitioning occurred, with juveniles, for example, living closer to the sea surface than later developmental

stages or vice versa. Modern studies show a range of different dispersal strategies in extant cephalopod paralarvae (Roura et al. 2019). A coastal dispersal pattern as seen, e.g., in the modern ommastrephids *Todaropsis eblanae* and *Illex coindeti* might be similar to the dispersal of the Late Devonian hatchlings with squid paralarvae staying between the coast and the limits of the continental shelf (Roura et al. 2019).

If all developmental stages of the Devonian ammonoids lived together, some problems like cannibalism might have occurred. Cannibalism has been documented for some Jurassic species (Schweigert and Dietl 1999; Keupp 2012; Ritterbush et al. 2014; Klug and Lehmann 2015; Hoffmann et al. 2020) and it is conceivable that ammonoids did not actively differentiate between their prey. Thus, consuming their own offspring when sharing the habitat is likely. Prey size played a key role and might constitute the main limitation for prey selection of most of the ammonoid species in our samples. With their small body sizes of mostly less than 40 mm and their low apertures of a few millimetres height (Korn and Klug 2012; Walton and Korn 2018), the majority of early Famennian ammonoids of the Tafilalt and Maïder would only have been able to feed on rather small prey. Relatively large eggs and hatchlings or fast-growing hatchlings might have helped to evade cannibalism. Ammonoid eggs are thought to have been only slightly larger than hatchlings and thus, their sizes can be approximated from the diameter of the embryonic conch (De Baets et al. 2012; Laptikhovsky et al. 2017).

In particular, the smallest specimens found in the early and middle Famennian samples of the Tafilalt and Maïder have a diameter of 1.0 mm, while the largest specimens reached a diameter of 32.5 mm (SOM 2). In the largest specimens, the aperture has a height of about 8 mm (calculated for incomplete specimens and measured for complete ones). With an aperture height of 8 mm, the maximum food size of an adult specimen was limited, because the prey size must have been much smaller. The average diameter of all ammonoids found within the studied samples is 10.1 mm including all the small hatchlings and juveniles (excluding Oum El Jerane). The maximum size of 32.5 mm was found only once among all specimens (except Oum El Jerane, SOM 2) and most ammonoids range between ca. 10 and 22 mm in diameter (SOM 2). The apertural height for this diameter range varies between ca. 2.3 mm and 5.1 mm (diameter divided by 4.2 in cheiloceratids of this ammonoid zone, Fig. 5C). Assuming that the hyponome, jaws and buccal musculature further reduced the gape (Mironenko 2014; Klug and Lehmann 2015; Klug et al. 2016; Walton and Korn 2018), the majority of the ammonoids of our samples could not have ingested prey larger than a few millimetres (< 1 mm prey size at a predator conch size of 10 mm and max. 3 mm at a predator conch size of around 20 mm). Additionally, if the Late Devonian ammonoids were semelparous like many modern cephalopods, adult individuals might have stopped feeding (at least, maximum prey size was further reduced by terminal constrictions of the conch) and the apertures and jaws of juvenile specimens were too small even to eat hatchlings. Cannibalism within the Late Devonian cheiloceratids, therefore, played probably only a subordinate role. Hatchlings sharing the habitat with the adults would have presented only a subordinate problem.

Conclusions

Five sediment samples of Famennian age from the eastern Anti-Atlas (Maïder and Tafilalt Basins with Tafilalt Platform) were examined. Two of these are stratigraphically assigned to the Famennian *Praemeroceras petterae* Zone, two are assigned to the middle Famennian *Maeneceras meridionale* Zone and one sample is assigned to the Famennian *Costaclymenia muensteri* Zone. All ammonoids were extracted from these samples, counted and measured. In order to estimate the total number of preserved ammonoids within a standard area of 1 km^2 and within the whole area and a layer thickness of 100 mm, several factors were estimated. The total surface of the two marine basins and the platform in between, the number and volume of all ammonoid conchs within each sample, the stratigraphic position and the approximate sedimentation rates.

The estimated numbers of ammonoids within the whole area with a layer thickness of 100 mm is estimated to range from 30.9×10^{13} to 19.4×10^{14} ammonoids and a annual conch accumulation of 15.4×10^{9} to 97.1×10^{10}. The annual biomass ranges from 25 954 to 47 058 t. These values have to be understood as estimates for the order of magnitude rather than exact measurements. We speculate that the actual numbers exceeded those we present here because of non-preservation, particularly of the smallest conchs. As the stratigraphic range is not known for all sampled layers and these mass occurrences might not have covered the whole area, the numbers for a standard area of 1 km^2 were estimated as well.

Several factors can lead to errors in the estimations as for example mistakes in the counts caused by the fact that very small ammonoids might have been overseen. Furthermore, the estimates can only give a hint to the number of formerly living ammonoids. Factors like the unknown preservation rate, laterally changing ammonoid abundances, taphonomy or recrystallisation can lead to differences between the number of preserved ammonoids and the number of ammonoids that have actually lived.

The samples were taken from layers with ammonoid mass occurrences. These accumulations of conchs can be caused by processes like sudden mass mortality or sedimentary processes such as transport, condensation and sorting. The presence of all ontogenetic stages in the samples supports the explanation of mass mortalities, but with some reservation. The above-mentioned sedimentary processes, however, are likely to damage the shells and some kind of sorting would occur where certain size-classes are over- or under-represented. This is not the case in all but one of our samples, where sedimentary processes probably caused the scarcity of juveniles (sorting, dissolution or else).

Actualistic comparisons to modern coleoid abundances help assessing the plausibility of the calculated numbers and biomass estimates. In fact, the biomass of Recent ommastrephid squids per area, for example, lies within the same order of magnitude. We stress here that the numbers we provide are intended to serve as a first attempt to quantify the order of magnitude of abundances. The obtained values coincide well with impressions we obtained during field work, namely that ammonoids played key roles in the marine food chains already in the Devonian, although it is poorly known, which predators relied on them as food source.

The large calculated number of ammonoids per area can partially be explained by the reproduction strategy of these ammonoids. We estimated an amount of 230 eggs per adult female based on the body chamber volumes and embryonic conch size. This moderately high reproduction rate can quickly lead to a high number of ammonoids providing the environmental conditions were favourable. We do not know the duration from hatching to maturity, but we assume that it did not exceed two years; possibly, it was shorter.

The size distribution found in the samples correspond roughly to the expected type III-survivorship curve of r-strategists with highly abundant hatchlings and early juveniles and exponentially decreasing abundances with size (roughly Gaussian distribution in logarithmic measures). Since most post-embryonic size classes were found in the samples, it appears unlikely that a geographical separation occurred between ontogenetic stages. By contrast, a vertical niche partitioning cannot be excluded. A geographical separation would have seemed expectable to avoid cannibalism, but this appears unlikely for the studied Late Devonian ammonoids as members of the most common size classes were probably unable to feed on hatchlings because of their rather small body and thus mouth sizes.

Acknowledgements

Thomas Imhof (Gebrüder Imhof Geowissenschaftliches Atelier, Trimbach, Switzerland) kindly prepared the sample shown in Fig. 1. We greatly appreciate the thorough and constructive reviews of Dieter Korn (Museum für Naturkunde, Berlin, Germany), René Hoffmann (RuhrUniversität Bochum, Germany), and Margaret M. Yacubucci (Bowling Green State University, USA). We thank the Swiss National Science Foundation for financial support (project nr. 200021_169627). Additionally, we acknowledge the Ministère de l'Energie, des Mines, de l'Eau et de l'Environnement (Direction du Développement Minier, Division du Patrimoine, Rabat, Morocco) for working and sample export permits.

References

Ait Daoud, M., Essalhi, A., Essalhi, M., and Toummite, A. 2019. The role of variscan shortening in the control of mineralization deposition in Tadaout-Tizi N'rsas mining district (Eastern Anti-Atlas, Morocco). *Bulletin of The Mineral Research and Exploration* 161: 13–32.

Alvaro, J.J., Benharref, M., Amrhar, A., Koukaya, A., and Jmili, A. 2014. *Carte géologique du Maroc, Al Atrous. Royaume du Maroc. Notes et Mémoires 555*. Service Géologique du Maroc, Rabat.

Andrews, P. 2006. Taphonomic effects of faunal impoverishment and faunal mixing. *Palaeogeography Palaeoclimatology Palaeoecology* 241: 572–589.

Baidder, L., Michard, A., Soulaimani, A., Fekkak, A., Eddebbi, A., Rjimati, E.-C., and Raddi, Y. 2016. Fold interference pattern in thick-skinned tectonics, a case study from the external Variscan belt of Eastern Anti-Atlas, Morocco. *Journal of African Earth Sciences* 119: 204–225.

Becker, R.T. 1993. Stratigraphische Gliederung und Ammonoideen-Faunen im Nehdenium (Oberdevon II) von Europa und Nord-Afrika. *Courier Forschungsinstitut Senckenberg* 155: 1–405.

Becker, R.T. 1995. Taxonomy and Evolution of late Famennian Tornoceratеae (Ammonoidea). *Berliner geowissenschaftliche Abhandlungen E* 16: 607–643.

Becker, R.T. and House, M.R. 2000a. Devonian ammonoid succession at Jbel Amelane (Western Tafilalt, Southern Morocco). *Notes et Mémoires Service Géologique du Maroc* 399: 49–56.

Becker, R.T. and House, M.R. 2000b. The Famennian ammonoid succession at Bou Tchrafine (Anti-Atlas, Southern Morocco). *Notes et Mémoires Service Géologique du Maroc* 399: 37–42.

Becker, R.T., Aboussalam, Z.S., Hartenfels, S., El Hassani, A., and Fischer, T. 2013. The Givetian–Famennian at Oum El Jerane (Amessoui syncline, southern Tafilalt). *In*: R.T. Becker, A. El Hassani, and A. Tahiri (eds.), *Excursion Guidebook "The Devonian and Lower Carboniferous of Northern Gondwana". Document de l'Institut Scientifique, Rabat* 27: 61–76.

Becker, R.T., Aboussalam, Z.S., Hartenfels, S., Gibb, A., Mayer, O., and Hüneke, H. 2018a. Emsian events, Frasnian–Famennian boundary, and *Gonioclymenia* Limestone at Jebel Ihrs (western Tafilalt Platform). *Münstersche Forschungen zur Geologie und Paläontologie* 110: 229–243.

Becker, R.T., El Hassani, A., Aboussalam, Z.S., Hartenfels, S., and Baidder, L. 2018b. The Devonian and Lower Carboniferous of the eastern Anti-Atlas: introduction to a 'cephalopod paradise'. *Münstersche Forschungen zur Geologie und Paläontologie* 110: 145–157.

Becker, R.T., Hartenfels, S., Klug, C., Aboussalam, Z.S., and Afhüppe, L. 2018c. The cephalopod-rich Famennian and Tournaisian of the Aguelmous Syncline (southern Maïder). *Münstersche Forschungen zur Geologie und Paläontologie* 110: 273–306.

Becker, R.T., House, M.R., Bockwinkel, J., Ebbighausen, V., and Aboussalam, Z.S. 2002. Famennian ammonoid zones of the eastern Anti-Atlas (southern Morocco). *Münstersche Forschungen zur Geologie und Paläontologie* 93: 159–205.

Becker, R.T., Marshall, J.E.A., Da Silva, A.-C., Agterberg, F.P., Gradstein, F.M., and Ogg, G.M. 2020. The Devonian period. *In*: F.M. Gradsteinand and G.M. Ogg (eds.), *Geologic Time Scale 2020*, 733–810. Elsevier, Amsterdam.

Belka, Z., Klug, C., Kaufmann, B., Korn, D., Döring, S., Feist, R., and Wendt, J. 1999. Devonian conodont and ammonoid succession of the eastern Tafilalt (Ouidane Chebbi section), Anti-Atlas, Morocco. *Acta Geologica Polonica* 49: 1–23.

Benharref, M., Alvaro, J.J., Jmili, A., and Boudad, L. 2014. Carte Géologique du Maroc. Irara. *Royaume du Maroc. Notes et Mémoires* 552. Service Géologique du Maroc, Rabat.

Boyle, P. 1983. *Cephalopod Life Cycles. Vol. 1, Comparative Reviews.* 441 pp. Academic Press, London.

Buggisch, W. 1991. The global Frasnian–Famennian "Kellwasser Event". *Geologische Rundschau* 80: 49–72.

Carmichael, R.S. 2017. *Practical Handbook of Physical Properties of Rocks and Minerals.* 2nd ed. 173 pp. CRC Press, Milton.

Chamberlain, J.A., Ward, P.D., and Weaver, J.S. 1981. Post-mortem ascent of *Nautilus* shells: implications for cephalopod paleobiogeography. *Paleobiology* 7: 494–509.

Chirat, R. 2000. The so-called "cosmopolitan palaeobiogeographic distribution" of Tertiary Nautilida of the genus *Aturia* Bronn 1838: the result of post-mortem transport by oceanic palaeocurrents. *Palaeogeography, Palaeoclimatology, Palaeoecology* 157: 59–77.

De Baets, K., Klug, C., Korn, D., and Landman, N.H. 2012. Early evo-

lutionary trends in ammonoid embryonic development. *Evolution* 66: 1788–1806.

De Baets, K., Landman, N.H., and Tanabe, K. 2015. Ammonoid embryonic development. *In*: C. Klug, D. Korn, K. De Baets, I. Kruta, and R.H. Mapes (eds.), Ammonoid Paleobiology: From Anatomy to Ecology. *Topics in Geobiology* 43: 113–205.

Döring, S. and Kazmierczak, M. 2001. Stratigraphy, geometry, and facies of a Middle Devonian ramp-to-basin transect (Eastern Anti-Atlas, SE Morocco). *Facies* 44: 137–150.

Doubleday, Z.A., Prowse, T.A., Arkhipkin A., Pierce, G.J., Semmens, J., Steer, M., Leporati, S.C., Lourenço, S., Quetglas, A., Sauer, W., and Gillanders, B.M. 2016. Global proliferation of cephalopods. *Current Biology* 26: R406–R407.

Doyle, P. and Macdonald, D.I.M. 1993. Belemnite battlefields. *Lethaia* 26: 65–80.

Frey, L. 2019. *A New Fossil-Lagerstätte from the Late Devonian of Morocco: Faunal Composition, Taphonomy, and Paleoecology*. 212 pp. Unpublished Ph.D. Thesis, University of Zurich, Zurich.

Frey, L., Naglik, C., Hofmann, R., Schemm-Gregory, M., Frýda, J., Kröger, B., Taylor, P.D., Wilson, M.A., and Klug, C. 2013. Diversity and palaeoecology of Early Devonian invertebrate associations in the Tafilalt (Anti-Atlas, Morocco). *Bulletin of Geosciences* 89: 75–112.

Frey, L., Pohle, A., Rücklin, M., and Klug, C. 2020. Fossil-Lagerstätten, palaeoecology and preservation of invertebrates and vertebrates from the Devonian in the eastern Anti-Atlas, Morocco. *Lethaia* 53: 242–266.

Frey, L., Rücklin, M., Korn, D., and Klug, C. 2018. Late Devonian and Early Carboniferous alpha diversity, ecospace occupation, vertebrate assemblages and bio-events of southeastern Morocco. *Palaeogeography, Palaeoclimatology, Palaeoecology* 496: 1–17.

Fuchs, D., Hoffmann, R., and Klug, C. 2021. Evolutionary development of the coleoid arm armature. *Swiss Journal of Palaeontology* 140 (27): 1–18.

Hartenfels, S. and Becker, R.T. 2018. The upper Famennian Dasberg Crisis and *Gonioclymenia* Limestone at Oum el Jerane (Amessoui Syncline, southern Tafilalt Platform). *Münstersche Forschungen zur Geologie und Paläontologie* 110: 261–272.

Hoffmann, R., Stevens, K., Keupp, H., Simonsen, S., and Schweigert, G. 2020. Regurgitalites—a window into the trophic ecology of fossil cephalopods. *Journal of the Geological Society* 177: 82–102.

Hollard, H. 1974. Recherches sur la stratigraphie des formations du Dévonien moyen, de l'Emsien supérieur au Frasnien, dans le Sud du Tafilalt et dans le Ma'der (Anti-Atlas oriental, Maroc). *Notes du Service Géologique du Maroc* 36: 7–4.

House, M.R. and Senior J.R. 1981. *The Ammonoidea. The Evolution, Classification, Mode of Life, and Geological Usefulness of a Major Fossil Group. Systematics Association Special Volume*. 594 pp. Academic Press, London.

Hoving, H.J.T., Bush, S.L., Haddock, S.H.D., and Robison, B.H. 2017. Bathyal feasting: post-spawning squid as a source of carbon for deep-sea benthic communities. *Proceedings of the Royal Society B* 284: 20172096.

Ikeda, Y. and Wani, R. 2012. Different modes of migration among Late Cretaceous ammonoids in northwestern Hokkaido, Japan: Evidence from the analyses of shell whorls. *Journal of Paleontology* 86: 605–615.

Jacobs, D.K. and Landman, N.H. 1993. *Nautilus*—a poor model for the function and behavior of ammonoids? *Lethaia* 26: 101–111.

Kaufmann, B. 1998. Facies, stratigraphy and diagenesis of Middle Devonian reef- and mud-mounds in the Mader (eastern Anti-Atlas, Morocco). *Acta Geologica Polonica* 48: 43–106.

Keupp, H. 2012. Atlas zur Paläopathologie der Cephalopoden. *Berliner Paläobiologische Abhandlungen* 12: 1–390.

Kidwell, S.M. and Bosence, D.W. 1991. Taphonomy and time-averaging of marine shelly faunas. *In*: P.A. Allison and D.E.G Briggs (eds.), Taphonomy: Releasing the Data Locked in the Fossil Record. *Topics in Geobiology* 9: 115–209.

Klug, C. 1997. *Stratigraphie, Fazies und Ammonoideen des Devons der Amessoui-Synklinale (östlicher Anti-Atlas, Marokko)*. 253 pp. Unpublished Diploma Thesis and Diploma Mapping, Institut und Museum für Geologie und Paläontologie der Eberhard-Karls-Universität, Tübingen.

Klug, C. 2001. Life-cycles of some Devonian ammonoids. *Lethaia* 34: 215–233.

Klug, C. and Lehmann, J. 2015. Soft part anatomy of ammonoids: reconstructing the animal based on exceptionally preserved specimens and actualistic comparisons. *In*: C. Klug, D. Korn, K. De Baets, I. Kruta, and R.H. Mapes (eds.), Ammonoid Paleobiology: From Anatomy to Ecology. *Topics in Geobiology* 43: 507–529.

Klug, C. and Pohle, A. 2018. The eastern Amessoui Syncline—a hotspot for Silurian to Carboniferous cephalopod research. *Münstersche Forschungen zur Geologie und Paläontologie* 110: 244–260.

Klug, C., Frey, L., Korn, D., Jattiot, R., and Rücklin, M. 2016. The oldest Gondwanan cephalopod mandibles (Hangenberg Black Shale, Late Devonian) and the mid-Palaeozoic rise of jaws. *Palaeontology* 59: 611–629.

Klug, C., Korn, D., De Baets, K., Kruta, I., and Mapes, R.H. (eds.) 2015a. Ammonoid Paleobiology. *Topics in Geobiology* 43, 1–947; 44, 1–610. Springer, Dordrecht.

Klug, C., Kröger, B., Vinther, J., Fuchs, D. and De Baets, K. 2015b. Ancestry, origin and early evolution of ammonoids. *In*: C. Klug, D. Korn, K. De Baets, I. Kruta, and R.H. Mapes (eds.), Ammonoid Paleobiology: from Macroevolution to Paleogeography. *Topics in Geobiology* 44: 3–24.

Klug, C., Schweigert, G., Tischlinger, H., and Pochmann, H. 2021. Failed prey or peculiar necrolysis? Isolated ammonite soft body from the Late Jurassic of Eichstätt (Germany) with complete digestive tract and male reproductive organs. *Swiss Journal of Palaeontology* 140 (3): 1–14.

Korn, D. 1999. Famennian ammonoid stratigraphy of the Ma'der and Tafilalt (Eastern Anti-Atlas, Morocco). *Abhandlungen der Geologischen Bundesanstalt* 54: 147–179.

Korn, D. and Klug, C. 2002. *Ammoneae devonicae*. *Fossilium catalogus. I, Animalia, pars 138*. 375 pp. Backhuys. Leiden.

Korn, D. and Klug, C. 2007. Conch form analysis, variability, and morphological disparity of a Frasnian (Late Devonian) ammonoid assemblage from Coumiac (Montagne Noire, France). *In*: N.H. Landman, R.A. Davis, W. Manger, and R.H. Mapes (eds.), *Cephalopods—Present and Past*, 57–86. Springer, New York.

Korn, D. and Klug, C. 2012. Palaeozoic ammonoids—diversity and development of conch morphology. *In*: J.A. Talent (ed.), *Earth and Life. Global Biodiversity, Extinction Intervals and Biogeographic Perturbations Through Time*, 491–534. Springer, Dordrecht.

Korn, D., Bockwinkel, J., and Ebbighausen, V. 2014. Middle Famennian (Late Devonian) ammonoids from the Anti-Atlas of Morocco. 1. *Prionoceras*. *Neues Jahrbuch für Geologie und Paläontologie Abhandlungen* 272: 167–204.

Korn, D., Bockwinkel, J., and Ebbighausen, V. 2015. Middle Famennian (Late Devonian) ammonoids from the Anti-Atlas of Morocco. 2. Sporadoceratidae. *Neues Jahrbuch für Geologie und Paläontologie Abhandlungen* 278: 47–77.

Korn, D., Bockwinkel, J., and Ebbighausen, V. 2016. Middle Famennian (Late Devonian) ammonoids from the Anti-Atlas of Morocco. 3. Tornoceratids. *Neues Jahrbuch für Geologie und Paläontologie Abhandlungen* 281: 267–281.

Korn, D., Bockwinkel, J., and Ebbighausen, V. 2018. Middle Famennian (Late Devonian) ammonoids from the Anti-Atlas of Morocco. 4. *Costaclymenia*. *Neues Jahrbuch für Geologie und Paläontologie Abhandlungen* 289: 35–41.

Korn, D., Klug, C., and Reisdorf, A. 2000. Middle Famennian ammonoid stratigraphy in the Amessoui Syncline (Late Devonian, eastern Anti-Atlas, Morocco). *Travaux de l'Institut Scientifique, Série Géologie & Géographie Physique* 20: 69–77:

Kröger, B., Vinther, J., and Fuchs, D. 2011. Cephalopod origin and evolution: A congruent picture emerging from fossils, development and molecules. *Bioessays* 33: 602–613.

Landman, N.H., Tanabe, K., and Davis, R.A. (eds.) 1996. *Ammonoid Paleobiology. Topics in Geobiology 13*. 857 pp. Plenum, New York.

Landman, N.H., Tanabe, K., and Shigeta, Y. 2013. Ammonoid embryonic

development. *In*: N.H. Landman, K. Tanabe, and R.A. Davis (eds.), Ammonoid Paleobiology. *Topics in Geobiology* 13: 343–405.

Laptikhovsky, V., Collins, M.A., and Arkhipkin, A.I. 2013. First case of possible iteroparity among coleoid cephalopods: the giant warty squid *Kondakovia longimana. Journal of Molluscan Studies* 79: 270–272.

Laptikhovsky, V., Nikolaeva, S., and Rogov, M. 2017. Cephalopod embryonic shells as a tool to reconstruct reproductive strategies in extinct taxa. *Biological Reviews* 93: 270–283.

Laptikhovsky, V.L., Rogov, M.A., Nikolaeva, S.E., and Arkhipkin, A.I. 2012. Environmental impact on ectocochleate cephalopod reproductive strategies and the evolutionary significance of cephalopod egg size. *Bulletin of Geosciences* 88: 83–94.

Lemanis, R., Zachow, S., Fusseis, F., and Hoffmann, R. 2015. A new approach using high-resolution computed tomography to test the buoyant properties of chambered cephalopod shells. *Paleobiology* 41: 313–329.

Lipiński, M.R. 1998. Cephalopod life cycles: patterns and exceptions. *South African Journal of Marine Science* 20: 439–447.

Llopis-Belenguer, C., Blasco-Costa, I., and Balbuena, J.A. 2018. Evaluation of three methods for biomass estimation in small invertebrates, using three large disparate parasite species as model organisms. *Science Reports* 8*:* 3897.

Lloyd, D. 1978. Adaptive value, entropy and survivorship curves. *Nature* 275: 213–214.

Lukeneder, S., Lukeneder, A., and Weber, G.W. 2014. Computed reconstruction of spatial ammonoid-shell orientation captured from digitized grinding and landmark data. *Computers & Geosciences* 64: 104–114.

Marshall, C.R., Latorre, D.V., Wilson, C.J., Frank, T.M., Magoulick, K.M., and Zimmt, J.B. 2021. Absolute abundance and preservation rate of Tyrannosaurus rex. *Science* 372: 284–287.

Mironenko, A.A. 2014. The soft-tissue attachment scars in Late Jurassic ammonites from Central Russia. *Acta Palaeontologica Polonica* 60: 981–1000.

Mironenko, A.A. and Rogov, M.A. 2016. First direct evidence of ammonoid ovoviviparity. *Lethaia,* 49: 245–260.

Munnecke, A. and Westphal, H. 2005. Variations in primary aragonite, calcite, and clay in fine-grained calcareous rhythmites of Cambrian to Jurassic age—an environmental archive? *Facies* 51: 592–607.

Naglik, C., Rikhtegar, F.N., and Klug, C. 2016. Buoyancy in Palaeozoic ammonoids from empirical 3D-models and their place in a theoretical morphospace. *Lethaia* 49: 3–12.

Nigmatullin, C.M. 2004. Estimation of biomass, production and fishery potential of ommastrephid squids in the world ocean and problems of their fishery forecasting. *International Council for the Exploration of the Sea* CM 2004/CC: 06.

Nigmatullin, C.M. and Markaida, U. 2009. Oocyte development, fecundity and spawning strategy of large sized jumbo squid *Dosidicus gigas* (Oegopsida: Ommastrephinae). *Journal of the Marine Biological Association of the United Kingdom* 89: 789–801.

Okamoto, T. 1996. Theoretical modeling of ammonoid morphology. *In*: N.H. Landman, K. Tanabe, K., and R.A. Davis (eds.), Ammonoid Paleobiology. *Topics in Geobiology* 13: 225–251.

Pohle, A., Fuchs, D., Korn, D., and Klug, C. 2020. Spatial distribution of oncocerid cephalopods on a Middle Devonian bedding plane suggests semelparous life cycle. *Scientific Reports* 10 (1): 2847.

Ricken, W. 1985. Epicontinental marl-limestone alternations: Event deposition and diagenetic bedding (upper Jurassic, southwest Germany). *In*: U. Bayer and A. Seilacher (eds.), Sedimentary and Evolutionary Cycles*. Lecture Notes in Earth Sciences* 1: 127–162.

Ricken, W. and Eder, W. 1991. Diagenetic modification of calcareous beds—an overview. *In*: G. Einsele, W. Ricken, and A. Seilacher (eds.), *Cycles and Events in Stratigraphy*, 430–449. Springer, Berlin.

Ritterbush, K.A., Hoffmann, R., Lukeneder, A., and De Baets, K. 2014. Pelagic palaeoecology: the importance of recent constraints on ammonoid palaeobiology and life history. *Journal of Zoology* 292: 229–241.

Robert-Charrue, C. and Burkhard, M. 2008. Inversion tectonics, interference pattern and extensional fault-related folding in the Eastern Anti-Atlas, Morocco. *Swiss Journal of Geoscience* 101: 397–408.

Rocha, F., Guerra, A., and González, A.F. 2001. A review of reproductive strategies in cephalopods. *Biological reviews of the Cambridge Philosophical Society* 76: 291–304.

Rodrigues, M., Garcí, M.E., Troncoso, J.S., and Guerra, Á. 2011. Spawning strategy in Atlantic bobtail squid *Sepiola atlantica* (Cephalopoda: Sepiolidae). *Helgoland Marine Research* 65: 43–49.

Roura, A., Amor, M., González, A.F., Guerra, A., Barton, E.D., and Strugnell, J.M. 2019. Oceanographic processes shape genetic signatures of planktonic cephalopod paralarvae in two upwelling regions. *Progress in Oceanography* 170: 11–27.

Schweigert, G. and Dietl, G. 1999. Zur Erhaltung und Einbettung von Ammoniten im Nusplinger Plattenkalk (Oberjura, Südwestdeutschland). *Stuttgarter Beiträge zur Naturkunde B* 272: 1–31.

Seilacher, A. 1970. Begriff und Bedeutung der Fossil-Lagerstätten. *Neues Jahrbuch für Geologie und Paläontologie Monatshefte* 1970 (1): 34–39.

Strasser, A. 2016. Hiatuses and condensation: an estimation of time lost on a shallow carbonate platform. *The Depositional Record* 1: 91–117.

Tajika, A., Landman, N.H., Hoffmann, R., Lemains, R., Morimoto, N., Ifrim, C., and Klug, C. 2020. Chamber volume development, metabolic rates, and selective extinction in cephalopods. *Scientific Reports* 10: 2950.

Tajika, A., Naglik, C., Morimoto, N., Pascual-Cebrian, E., Hennhöfer, D.K., and Klug, C. 2015. Empirical 3D-model of the conch of the Middle Jurassic ammonite microconch *Normannites*, its buoyancy, the physical effects of its mature modifications and speculations on their function. *Historical Biology* 27: 181–191.

Tajika, A., Nützel, A., and Klug, C. 2018. The old and the new plankton: ecological replacement of associations of mollusc plankton and giant filter feeders after the Cretaceous? *PeerJ* 6: e4219.

Tawadros, E.E. 2018. *Geology of North Africa*. 930 pp. CRC Press, Boca Raton.

Toto, E.A., Kaabouben, F., Zouhri, L., Belarbi, M., Benammi, M., Hafid, M., and Boutib, L. 2008. Geological evolution and structural style of the Palaeozoic Tafilalt sub-basin, eastern Anti-Atlas (Morocco, North Africa). *Geological Journal* 43: 59–73.

Vijai, D., Sakai, M., Kamei, Y., and Sakurai, Y. 2014. Spawning pattern of the neon flying squid *Ommastrephes bartramii* (Cephalopoda: Oegopsida) around the Hawaiian Islands. *Scientia Marina* 78: 511–519.

Walton, S.A. and Korn, D. 2018. An ecomorphospace for the Ammonoidea. *Paleobiology* 44: 273–289.

Walton, S.A., Korn, D., and Klug, C. 2010. Size distribution of the Late Devonian ammonoid *Prolobites*: indication for possible mass spawning events. *Swiss Journal of Geoscience* 103: 475–494.

Wani, R., Kase, T., Shigeta, Y., and de Ocampo, R. 2005. New look at ammonoid taphonomy, based on field experiments with modern chambered Nautilus. *Geology* 33: 849–852.

Wendt, J. 1985. Disintegration of the continental margin of northwestern Gondwana: Late Devonian of the eastern Anti-Atlas (Morocco). *Geology* 13: 815–818.

Wendt, J. 1988. Condensed carbonate sedimentation in the late Devonian of the eastern Anti-Atlas (Morocco). *Eclogae Geologicae Helvetiae* 1: 81.

Wendt, J. 2021a. Middle and Late Devonian paleogeography of the eastern Anti-Atlas (Morocco). *International Journal of Earth Science* 110: 1531–1544.

Wendt, J. 2021b. Middle and Late Devonian sea-level changes and synsedimentary tectonics in the eastern Anti-Atlas (Morocco). *Journal of African Earth Sciences* 182: 104247.

Wendt, J. and Aigner, T. 1985. Facies patterns and depositional environments of Palaeozoic cephalopod limestones. *Sedimentary Geology* 44: 263–300.

Wendt, J. and Belka, Z. 1991. Age and depositional environment of Upper Devonian (early Frasnian to early Famennian) black shales and limestones (Kellwasser facies) in the eastern Anti-Atlas, Morocco. *Facies* 25: 51–89.

Wendt, J., Aigner, T., and Neugebauer, J. 1984. Cephalopod limestone deposition on a shallow pelagic ridge: the Tafilalt Platform (upper Devonian, eastern Anti-Atlas, Morocco). *Sedimentology* 31: 601–625.

Yacobucci, M.M. 2018. Post mortem transport in fossil and modern shelled cephalopods. *PeerJ* 6: e5909.